

<b>Title</b>	<b>Bone turnover and articular cartilage differences localized to subchondral cysts in knees with advanced osteoarthritis</b>
<b>Author(s)</b>	<b>Chen, Y; Wang, T; Guan, M; Zhao, W; Leung, FKL; Pan, H; Cao, X; Guo, XE; Lu, WW</b>
<b>Citation</b>	<b>Osteoarthritis and Cartilage, 2015, v. 23 n. 12, p. 2174-2183</b>
<b>Issued Date</b>	<b>2015</b>
<b>URL</b>	<b><a href="http://hdl.handle.net/10722/231201">http://hdl.handle.net/10722/231201</a></b>
<b>Rights</b>	<b>This work is licensed under a Creative Commons Attribution-NonCommercial-NoDerivatives 4.0 International License.</b>

# Osteoarthritis and Cartilage



## Bone turnover and articular cartilage differences localized to subchondral cysts in knees with advanced osteoarthritis

Y. Chen †¶<sup>a</sup>, T. Wang ‡<sup>a</sup>, M. Guan ‡, W. Zhao †, F-K-L. Leung †§, H. Pan ‡, X. Cao ‡||, X.E. Guo ‡¶, W.W. Lu †‡§\*

† Department of Orthopaedics and Traumatology, The University of Hong Kong, Hong Kong

‡ Center for Human Tissue and Organs Degeneration and Shenzhen Key Laboratory of Marine Biomedical Materials, Shenzhen Institutes of Advanced Technology, CAS, China

§ Shenzhen Key Laboratory for Innovative Technology in Orthopaedic Trauma, The University of Hong Kong Shenzhen Hospital, China

|| Department of Orthopaedic Surgery, Johns Hopkins University School of Medicine, Baltimore, MD, USA

¶ Bone Bioengineering Laboratory, Department of Biomedical Engineering, Columbia University, New York, USA

### ARTICLE INFO

#### Article history:

Received 4 March 2015

Accepted 21 July 2015

#### Keywords:

Osteoarthritis  
Subchondral bone cyst  
Bone remodeling  
Bone structure  
Articular cartilage

### SUMMARY

**Objective:** To investigate changes in bone structure, turnover, and articular cartilage localized in subchondral bone cyst (SBC) regions associated with knee osteoarthritis (OA).

**Methods:** Tibial plateaus ( $n = 97$ ) were collected from knee OA patients during total knee arthroplasty (TKA). SBCs were identified using micro-computed tomography, and the specimens were divided into non-cyst ( $n = 25$ ) and bone cyst ( $n = 72$ ) groups. Microstructure of subchondral bone was assessed using bone volume fraction (BV/TV), trabecular number (Tb.N), structure model index (SMI) and bone mineral density (BMD). In bone cyst group, the cyst subregion, which contained at least one cyst, and the peri-cyst subregion, which contained no cysts, were further selected for microstructure analysis. Articular cartilage damage was estimated using the Osteoarthritis Research Society International (OARSI) score. The numbers of TRAP<sup>+</sup> osteoclasts, Osterix<sup>+</sup> osteoprogenitors, Osteocalcin<sup>+</sup> osteoblasts and expression of SOX9 were evaluated by immunohistochemistry.

**Results:** Bone cyst group presented higher BV/TV, Tb.N and SMI at subchondral bone than non-cyst group. Furthermore, cyst subregion displayed increased BV/TV and Tb.N but lower BMD and SMI than peri-cyst subregion. Histology revealed a higher OARSI score in bone cyst group. SBC exhibited a weak relationship with BV/TV, etc. The numbers of TRAP<sup>+</sup> osteoclasts, Osterix<sup>+</sup> osteoprogenitors, Osteocalcin<sup>+</sup> osteoblasts and expression of SOX9, were higher in bone cyst group.

**Conclusion:** SBCs within knee OA are characterized by focally increased bone turnover, altered bone structure and more severe articular cartilage damage. The increased bone turnover possibly contributes to altered bone structure localized in SBC areas, and thus aggravates articular cartilage degeneration.

© 2015 Osteoarthritis Research Society International. Published by Elsevier Ltd. All rights reserved.

### Introduction

Osteoarthritis (OA) is one of the most prevalent joint disorders characterized by articular cartilage attrition and joint pain.

Nowadays, OA is considered a disease of “the whole joint”<sup>1,2</sup>. The integrity and function of the cartilage can be influenced by pathological changes in structure and function of other joint tissues. Focal interaction among subchondral bone, marrow and cartilage in OA pathogenesis is drawing increasing attention<sup>3–6</sup>.

Subchondral bone cysts (SBCs) were first defined as a concentric arrangement of trabeculae around an enlarged marrow space on radiographs<sup>7,8</sup>. On magnetic resonance imaging (MRI), SBCs demonstrate well-defined rounded areas of fluid-like signal intensity<sup>9,10</sup>. This allows the detection of small SBCs, and thus MRI is more sensitive than radiography in detecting SBCs<sup>9</sup>. Through the use of MRI, it has been reported that SBCs are present in up to 57% of OA patients<sup>11</sup>. The presence of SBCs is associated with knee

\* Address correspondence and reprint requests to: W.W. Lu, Department of Orthopaedics and Traumatology, The University of Hong Kong, Room 907, Lab Block, 21 Sassoon Road, Hong Kong. Tel: 852-2819-9595; Fax: 852-2818-5210.

E-mail addresses: cy003@hku.hk (Y. Chen), wangting@siat.ac.cn (T. Wang), min.guan@siat.ac.cn (M. Guan), zhaoww@hku.hk (W. Zhao), kllleunga@hkucc.hku.hk (F-K-L. Leung), hb.pan@siat.ac.cn (H. Pan), xcao11@jhmi.edu (X. Cao), exg1@columbia.edu (X.E. Guo), wwlu@hku.hk (W.W. Lu).

<sup>a</sup> These authors contributed equally to this manuscript.

pain<sup>12</sup>, joint disability<sup>13</sup>, cartilage loss, and increased risk of knee replacement in OA<sup>14</sup>. Two theories were supposed to explain the formation of SBCs: the “fluid breach theory”<sup>15</sup>, and the “bony contusion theory” which claimed that, in the region of subchondral bone where the overloading exceeds the limits of physiological endurance, the bone dies and is liquefied<sup>16,17</sup>. SBCs were reported to develop in bone marrow lesions (BMLs) in patients with or at risk for knee OA, which supports the bony contusion theory<sup>10</sup>. Using micro computed tomography (micro-CT), studies revealed that trabeculae around SBCs was increased in density but decreased in mineralization than trabeculae unaffected by SBCs in human hip OA<sup>15,16</sup>. However, such changes have not been fully elucidated in human knee OA.

Histologically, necrotic bone fragments in SBCs and fibrous tissue surrounding cyst cavities were found in human OA knee<sup>18</sup>. Furthermore, immunohistochemical staining showed high expression of markers for osteoblast and osteoclast in SBCs in an animal model of secondary knee OA<sup>19</sup>. These studies suggest that changes in bone structure and remodeling occur in SBC regions. However, histopathology evaluation of cartilage and bone remodeling in SBCs within human knee OA are still poorly understood. Investigation of associations among bone remodeling and structure and cartilage in SBC regions will contribute to knowledge of OA pathogenesis.

Thus, we aimed to determine the changes in bone structure and turnover, and cartilage, within the SBC regions. We intended to identify the possible association between SBC formation and cartilage degeneration in the same subregions. By determining the contents within and surrounding SBCs, we hoped to provide insight into the origin of OA SBCs. We hypothesized that SBC regions in human OA knees are foci of increased bone remodeling and altered structure, and are spatially associated with articular cartilage degradation.

## Patients and methods

### Subjects

This study was approved by the Institution Review Board of the University of Hong Kong (Ref Nr: UW-09368). All patients gave informed written consent prior to their participation in this study.

A consecutive series of 97 patients with primary knee OA was enrolled in this study at the authors' hospital from February 2012 to April 2013. The diagnosis of OA was according to the classification of the American College of Rheumatology<sup>20</sup>. Inclusion criteria were Chinese living in Hong Kong aged between 45 and 75 years old. Patients were excluded if they had a history of knee joint trauma, other forms of arthritis, metabolic bone diseases, bone tumors, or were on any medications affecting bone remodeling. The patients' demographic data, including age, sex, and body mass index (BMI), were recorded. The large SBCs were observed using plain radiographs. The radiographic severity of OA were evaluated according to Kellgren and Lawrence (K–L) system<sup>21</sup> by an experienced reader (FL), using radiographs (standing anteroposterior view in 15° of flexion and a supine lateral view in 45° of flexion)<sup>22</sup> obtained 1 week prior to operation. Mechanical alignment of the lower extremity (the hip-knee-ankle angle) was assessed with full-limb standing radiographs (FL)<sup>23</sup>. The radiograph reader was blinded to patients' other information while performing K–L grading and assessment of mechanical alignment.

### Micro-CT

Tibial plateaus removed from the 97 patients during total knee arthroplasty (TKA) were collected. Then, macroscopic examination of these specimens was performed. Serial micro-CT scans of these 97 tibial specimens were carried out under a micro-CT scanner

(Bruker micro-CT 1076, Belgium) with protocols described previously<sup>24</sup>. For three dimensional (3-D) measurements, the volume of interest (VOI) was selected as  $10 \times 10 \times 5 \text{ mm}^3$  of trabecular bone beneath the subchondral plate (SP) at the center of the medial tibial plateau (Supplementary Fig. 2A–D). The extraction of subchondral bone was performed with the aid of the edge detection function of MAT-LAB R2010a as previously described<sup>24</sup>. Briefly, the 2-D images were converted into discrete binary objects by the global thresholding and binarisation procedures using the software CTAn (Bruker micro-CT, Belgium). The irregular boundary of binary objects was detected after segmentation. The edges of bone cyst were saved as the region of interest (ROI) in the binary bitmap images, and unwanted edges were removed based on their coordinates in the segmented images to obtain the ROI for analysis.

The presence of SBCs was examined in all three anatomical planes using the software DataViewer (Bruker micro-CT, Belgium) (Supplementary Fig. 1). A bone cyst was defined as a spherical or ellipsoidal space that contained hardly any bone<sup>15,16</sup>. Only SBCs with a diameter greater than 1 mm were extracted, using an automatic method proposed by Chiba and colleagues<sup>25,26</sup> with the “morphology-based operations” model of the software CTAn. Briefly, trabeculae were dilated by 0.5 mm from the surface three-dimensionally, so bone marrow spaces less than 1 mm in diameter were closed. Next, the remaining spaces were dilated by 0.5 mm from the surfaces to restore their original shape. Then, after confirming the shape of the spaces (spherical or ellipsoidal), the SBCs were obtained<sup>25,26</sup>. Then the volume of SBCs was analyzed with the software CTAn. According to the absence or presence of SBCs, the subjects were divided into two groups: a non-cyst group ( $n = 25$ ) and a bone cyst group ( $n = 72$ ).

We further selected three subregions from the two selected VOIs in each of the two groups (Fig. 2a). Each subregion contained cylindrical subchondral bone of 3 mm in diameter and 10 mm in height. The three subregions were the “cyst” subregion, which contained at least one SBC ( $n = 23$ ); the peri-cyst subregion, which was 3 mm adjacent to the cyst subregion in the same specimen and contained no bone cyst ( $n = 23$ ); and the matched subregion, which is consistent with the anatomic location of cyst subregion ( $n = 25$ ). If a peri-cyst subregion was not able to be selected, the specimen was excluded.

Then three dimensional (3-D) analysis of subchondral bone was performed using the software CTAn. The following parameters were calculated: bone volume fraction (BV/TV), trabecular number (Tb.N), trabecular thickness (Tb.Th), trabecular separation (Tb.Sp), trabecular pattern factor (Tb.Pf)<sup>27</sup>, structure model index (SMI)<sup>28</sup>, degree of anisotropy (DA) and connectivity density (Conn.D). Moreover, the bone mineral density (BMD) was calibrated by using the attenuation coefficient of two hydroxyapatite phantoms (supplied by Bruker micro-CT, Belgium) with defined BMD of  $0.25 \text{ g/cm}^3$  and  $0.75 \text{ g/cm}^3$ . The BMD color maps were established using the software CTvox (Bruker micro-CT, Belgium).

### Histology

After the micro-CT scan, tissue plugs corresponding to the VOIs of tibial plateaus ( $n = 15$ ; samples were randomly selected from each group) were further processed for histological analysis. Serial sections were made into 5- $\mu\text{m}$  thicknesses and stained with hematoxylin and eosin as well as Safranin O and Fast Green. Cartilage and subchondral bone regions were observed under light microscopy (Olympus DP 80). OA cartilage pathology was evaluated using the Osteoarthritis Research Society International (OARSI) scoring method<sup>29</sup>. Evaluations were conducted by an experienced expert (TW) blinded to the findings from radiographs, micro-CT and medical records. The ratio of bone area to total area of subchondral

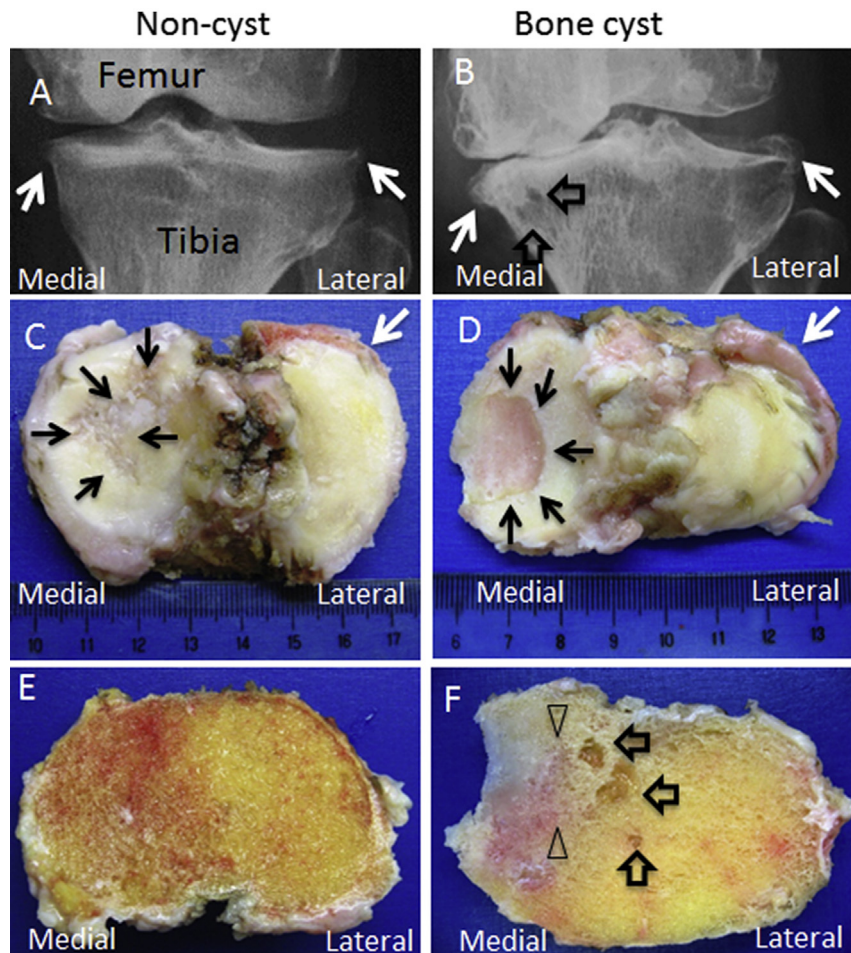


**Fig. 1. Radiographic and macroscopic view of osteoarthritic tibial plateaus without or with SBCs.** SBCs were noted in plain radiographs (black hollow arrows in B). Worn-out cartilage (black arrows) was indicated in the two groups (C and D). Osteophytes were noted in tibial plateaus in both groups (white arrows, A–D). Large bone cysts (black hollow arrows in F) were noted in macroscopic view. Sclerotic subchondral bone was observed in areas adjacent to bone cysts (arrow heads in F).

bone was assessed by Image-Pro Plus version 5.0 (Media Cybernetics, Inc.) as previously described<sup>3,4</sup>. Briefly, at least five sections from each sample were stained for analysis. For each section, five areas were measured<sup>3,4</sup>.

#### Immunohistochemistry

Biomarkers of osteoclast (tartrate-resistant acidic phosphatase, TRAP), osteoblast (Osteocalcin), osteoprogenitor (Osterix)<sup>3,4</sup>, and biomarkers of the chondrogenic phase during endochondral bone formation (SOX9)<sup>30</sup> were detected using immunohistochemistry with protocols described previously ( $n = 15$ ; samples were randomly selected from each group)<sup>3,4,31</sup>. TRAP staining was performed according to the manufacturer's protocol (Sigma). Other sections were incubated overnight with either anti-Osterix (Abcam), anti-Osteocalcin (TakaRa), or anti-SOX9 (Abcam) primary antibodies, followed by horseradish peroxidase-labeled secondary antibodies (Abcam) and developed with 3, 3'-diaminobenzidine substrate (Vector Laboratories). After image capture, the number of positive cells was quantified as previously described by a blinder (MG)<sup>3,4</sup>.

#### Statistical analysis

The epidemiological, micro-CT, histology and immunohistochemistry data were tested for normality using Shapiro–Wilk Test.

The comparison of the variables between the non-cyst and bone cyst groups was conducted using the Student's *t*-test for normally distributed variables and the chi-square test for categorical data (i.e., gender and K–L grade). Correlations of SBC volume with subchondral bone microstructure parameters and OARSI score were estimated using the Pearson's correlation coefficient test. The comparison of micro-CT variables among the cyst, peri-cyst and matched subregions was performed using one-way ANOVA. If the result was significant, a post-hoc test was further conducted. Statistical significance was set as  $P < 0.05$ . SPSS 20.0 (Chicago, IL) was used for all statistical analyses.

#### Results

##### Patient demographics

Of the 97 patients enrolled, 74.2% (72 of 97) had SBCs. No statistically significant differences were found between the two groups regarding the patients' gender, age, BMI, or alignment angle ( $P$  values range from 0.201 to 0.562; see [Supplementary Table](#)). Regarding K–L grade, there were 3 patients with grade 2, 6 patients with grade 3, and 16 patients with grade 4 in non-cyst group. In bone cyst group, there was 1 patient with grade 2, 24 patients with grade 3 and 47 patients with grade 4. The two groups showed marginally significant difference in the K–L grade ( $P = 0.061$ ).

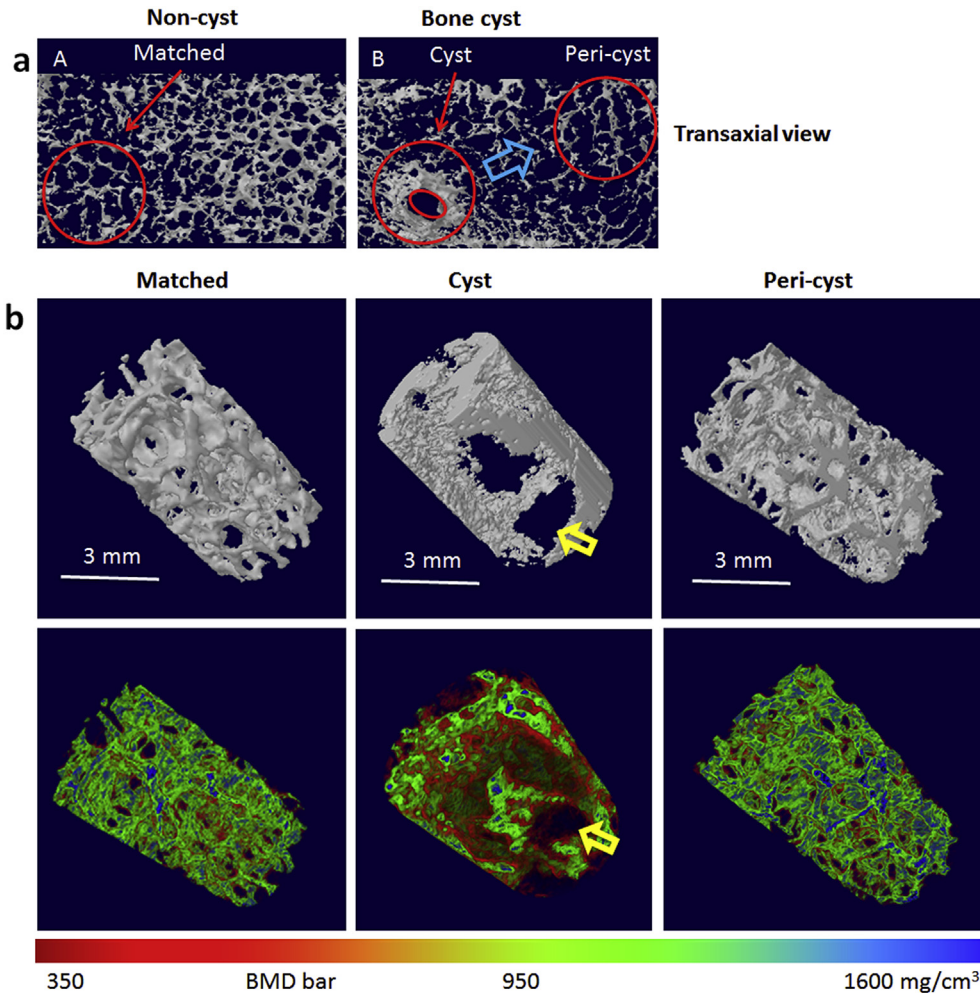


**Fig. 2.** Comparison of microstructure and degree of mineralization among subregions from subchondral bone with or without bone cysts. (a). From the VOIs of the non-cyst and bone cyst groups, three cylindrical subregions (3 mm in diameter and 10 mm in height) were selected: the cyst subregion (containing SBCs), peri-cyst subregion (3 mm away from cyst subregion in the same specimen and not containing SBCs) and matched subregion (consistent with anatomic location of cyst subregion). (b). The micro-CT 3-D images and BMD maps with BMD bar of the three subregions are displayed. Note the SBCs in the cyst subregion (arrows).

In plain radiographs, SBCs were observed in tibial plateaus of the bone cyst group (Fig. 1A and B). Under macroscopic view, large SBCs were observed in the tibial plateaus (Fig. 1D). Sclerotic subchondral bone was noted surrounding the SBCs (Fig. 1F).

#### Micro-CT

The micro-CT 3-D images of the non-cyst and bone cyst groups are displayed in Supplementary Fig. 2A–L. The BMD in the subchondral bone around the SBCs was demonstrated in the color maps (Supplementary Fig. 2M–P). Quantitative analysis revealed that the bone cyst group had an average cyst volume of  $5.18 \pm 3.85 \text{ mm}^3$  (range from 2.19 to  $21.97 \text{ mm}^3$ ). Subchondral bone within the bone cyst group had significantly higher BV/TV (34.9% higher,  $P = 0.003$ ), Tb.N (35.0%,  $P = 0.017$ ) and lower SMI (–43.8%,  $P = 0.001$ ) compared with the non-cyst group (Supplementary Fig. 3). No statistically significant difference was found in DA, Conn.D, Tb.Th, Tb.Sp, Tb.Pf or BMD ( $P$  values range from 0.125 to 0.229), between the two groups. Significant correlations of bone cyst volume with BV/TV ( $P = 0.010$ ), Tb.N ( $P = 0.029$ ), SMI ( $P < 0.001$ ), DA ( $P = 0.001$ ), and Tb.Pf ( $P < 0.001$ ) were found using the Pearson's correlation coefficient test (Table 1). No significant correlations of bone cyst volume were found with Tb.Th or Tb.Sp (both  $P$  values  $> 0.500$ ).

The micro-CT 3-D images and BMD maps of the matched, cyst, and peri-cyst subregions are displayed in Fig. 2b. The one-way ANOVA shows that there were statistically significant differences in BV/TV ( $P = 0.009$ ), Tb.N ( $P = 0.026$ ), BMD ( $P = 0.041$ ), SMI ( $P = 0.029$ ), and Tb.Sp ( $P = 0.045$ ) among the three subregions (Fig. 3). No statistically significant differences among subregions were found in Tb.Th, DA, Conn.D or Tb.Pf ( $P$  values range from 0.131 to 0.273) of the subchondral trabecular bone. Post-hoc tests showed that the cyst subregion was higher in BV/TV ( $P < 0.001$ ) and Tb.N ( $P < 0.002$ ), but lower in BMD ( $P < 0.037$ ) and SMI ( $P < 0.001$ ), than the matched and the peri-cyst subregions. The matched subregion was higher in Tb.Sp than the cyst and the peri-cyst subregions ( $P < 0.041$ ). In addition, no statistically significant differences in BV/TV, BMD, Tb.N, or SMI ( $P$  values range from 0.690 to 0.806) were found between the matched and the peri-cyst subregions.

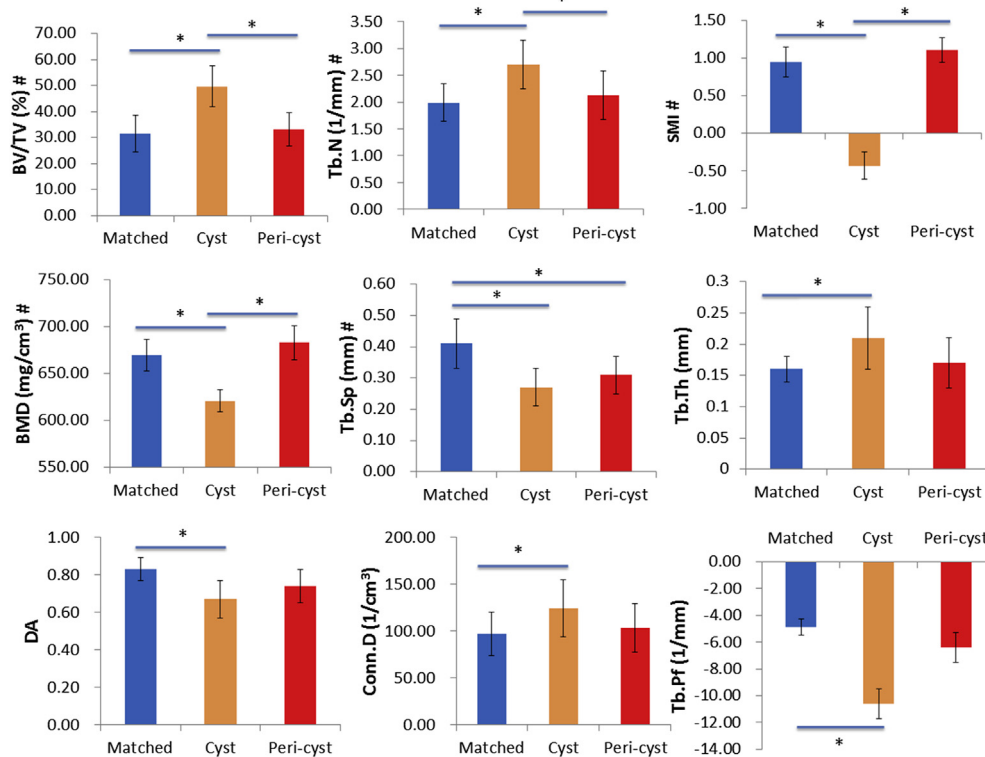
#### Histology

The worn-out articular cartilage in the non-cyst and bone cyst groups is shown in Fig. 4. Quantitative analysis revealed significantly higher OARSI scores in the bone cyst group than non-cyst group ( $20 \pm 3$  for bone cyst group and  $12 \pm 2$  for non-cyst group,  $P < 0.001$ , Fig. 4I). Furthermore, SBC volume positively correlated

**Table 1**

Correlations between SBC volume and bone microstructure and degree of mineralization and cartilage degeneration of tibial plateaus from knee OA patients

	BV/TV	Tb.N	Tb.Th	Tb.Sp	Tb.Pf	SMI	DA	Conn.D	BMD	OARSI score	
Bone cyst volume	<i>r</i>	0.407	0.342	0.087	-0.021	-0.516	-0.541	-0.488	0.186	-0.110	0.511
	<i>p</i>	<b>0.010</b>	<b>0.029</b>	0.591	0.897	<b>&lt;0.001</b>	<b>&lt;0.001</b>	<b>0.001</b>	0.251	0.497	<b>0.003</b>

The correlations were performed using Pearson's correlation coefficient. Bold text indicates a statistically significant correlation with a *P* value less than 0.05.**Fig. 3. Quantitative analysis of microstructure and mineralization among three subregions from subchondral bone with or without bone cysts.** # = parameter with significant difference among subregions using one-way ANOVA ( $P < 0.05$ ). \* = significant difference between two subregions according to post-hoc tests ( $P < 0.05$ ).

with OARSI scores ( $r = 0.511$ ,  $P = 0.003$ , Table 1). Compared with the non-cyst group, some areas of the SP in the bone cyst group were occupied by focal fibrocartilage tissue. Fibrocartilage tissue was also observed at the edges of the SBCs. In addition, large amounts of fibrous tissue were also noted in bone cyst cavities (Fig. 4D and H). Trabecular bone fragments without viable osteocytes within the bone cyst cavity were observed in the bone cyst group (Fig. 4D and H), indicating focal bone necrosis. Quantitative analysis revealed a statistically higher (37.5%;  $P = 0.011$ ) ratio of bone area/total area in the bone cyst group compared with the non-cyst group (Fig. 4J).

### Immunohistochemistry

Quantitative analysis revealed a significantly higher number of TRAP<sup>+</sup> osteoclasts in the bone cyst group compared with the non-cyst group ( $P = 0.003$ , Fig. 5). Osterix<sup>+</sup> osteoprogenitors in the bone cyst group aggregated around the SBCs, while Osterix<sup>+</sup> osteoprogenitors in the non-cyst group were mainly distributed in bone marrow (Fig. 6a). Quantitative analysis showed a significantly higher number of the Osterix<sup>+</sup> osteoprogenitors in the bone cyst group ( $P = 0.017$ ; Fig. 6b). Similarly, Osteocalcin<sup>+</sup> osteoblasts were obviously noted at the cyst wall (Fig. 6c). Quantitative analysis also revealed a significantly higher number of Osteocalcin<sup>+</sup> osteoblasts

in the bone cyst group (Fig. 6d), suggesting elevated level of osteoblastogenesis. Taken together, these findings indicate increased subchondral bone turnover in the bone cyst group compared with the non-cyst group.

Immunohistochemistry of SOX9 revealed a significantly higher number of SOX9<sup>+</sup> cells in the bone cyst group, indicating elevated endochondral bone formation compared with the non-cyst group. Additionally, the SOX9<sup>+</sup> cells in the bone cyst group were observed mainly at the wall of the bone cyst (Fig. 7).

### Discussion

In this study, we investigated changes in bone remodeling, bone structure and articular cartilage associated with SBCs within human knee OA. We found that bone and articular cartilage demonstrate changes localized to SBC regions. These findings support the paradigm of focal interactions among bone, marrow, and articular cartilage in pathogenesis of knee OA.

Studies using MRI have reported that knee OA patients have enlarged SBCs and develop new SBCs as the disease progresses<sup>10,14</sup>. In this study, the frequency of SBCs (74%) in OA patients was higher than that (57%) reported in a previous study using MRI<sup>11</sup>. One possible reason for such a discrepancy was that the patients in our

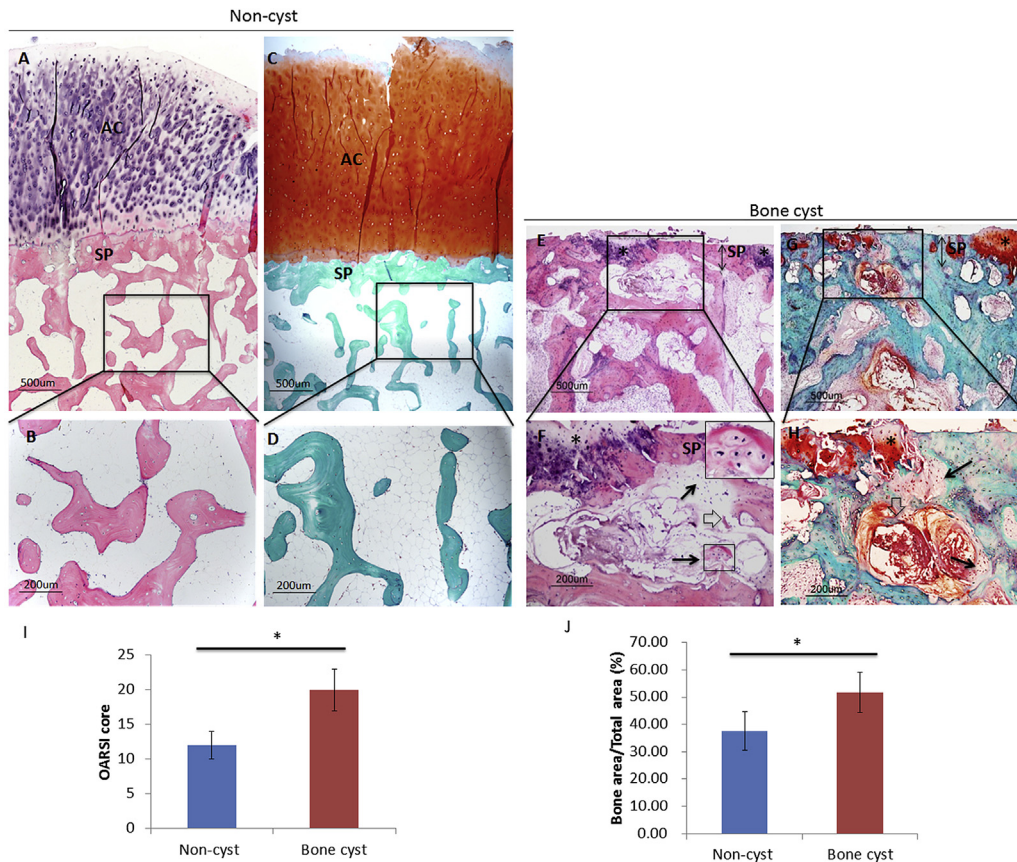


**Fig. 4. Histological images of tibial subchondral bone without or with bone cysts.** Articular cartilage (AC) could be observed in the non-cyst group (A and C). In contrast, most of the articular cartilage was worn-out in the bone cyst group (E and G). Compared with the non-cyst group, some areas of the SP in the bone cyst group were occupied by focal fibrocartilage tissue (\* in E–H). Fibrocartilage tissue was also observed at the edge of the cysts (arrows, F and H). Large amounts of fibrous tissue were noted in bone cyst cavities. Trabecular bone fragments without osteocytes imbedded were observed in the bone cyst group (hollow arrows, F and H), indicating focal bone necrosis. The OARSI score was significantly higher in bone cyst group compared with the non-cyst group (I). The ratio of bone area to total area in the bone cyst group was significantly higher (J). \* =  $P < 0.05$ .

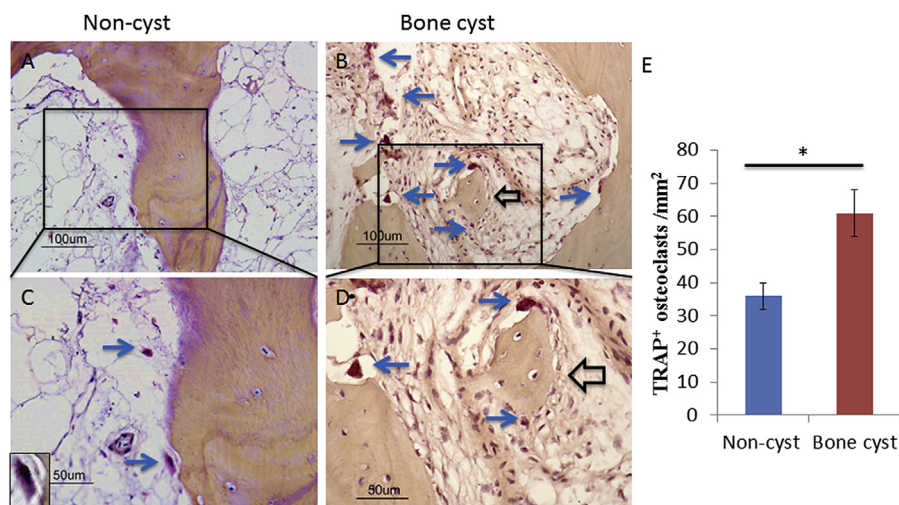


**Fig. 5. Higher activity of osteoclasts in subchondral bone with bone cysts than without bone cysts.** Compared with the non-cyst group (A and C), in the bone cyst group, bone fragments (black hollow arrows in B and D) were observed within the cyst cavity. TRAP<sup>+</sup> Osteoclasts (blue arrows) surrounding bone fragments were noted within SBC. A significantly larger number of TRAP<sup>+</sup> osteoclasts were detected in the subchondral bone of the bone cyst group, indicating increased bone resorption, compared with the non-cyst group (E). \* =  $P < 0.05$ .

study were in advanced stages of OA (mainly grade 3 or 4 on the K–L scale), while patients of that study were in relatively early stages of OA ( $\leq$  grade 3 on the K–L scale)<sup>11</sup>. Thus, our results are consistent with previous studies<sup>10,14</sup>. No significant difference was

found in epidemiological data between the non-cyst and bone cyst groups, indicating that these factors do not interfere with the comparison of subchondral bone ultrastructure and remodeling between the two groups.

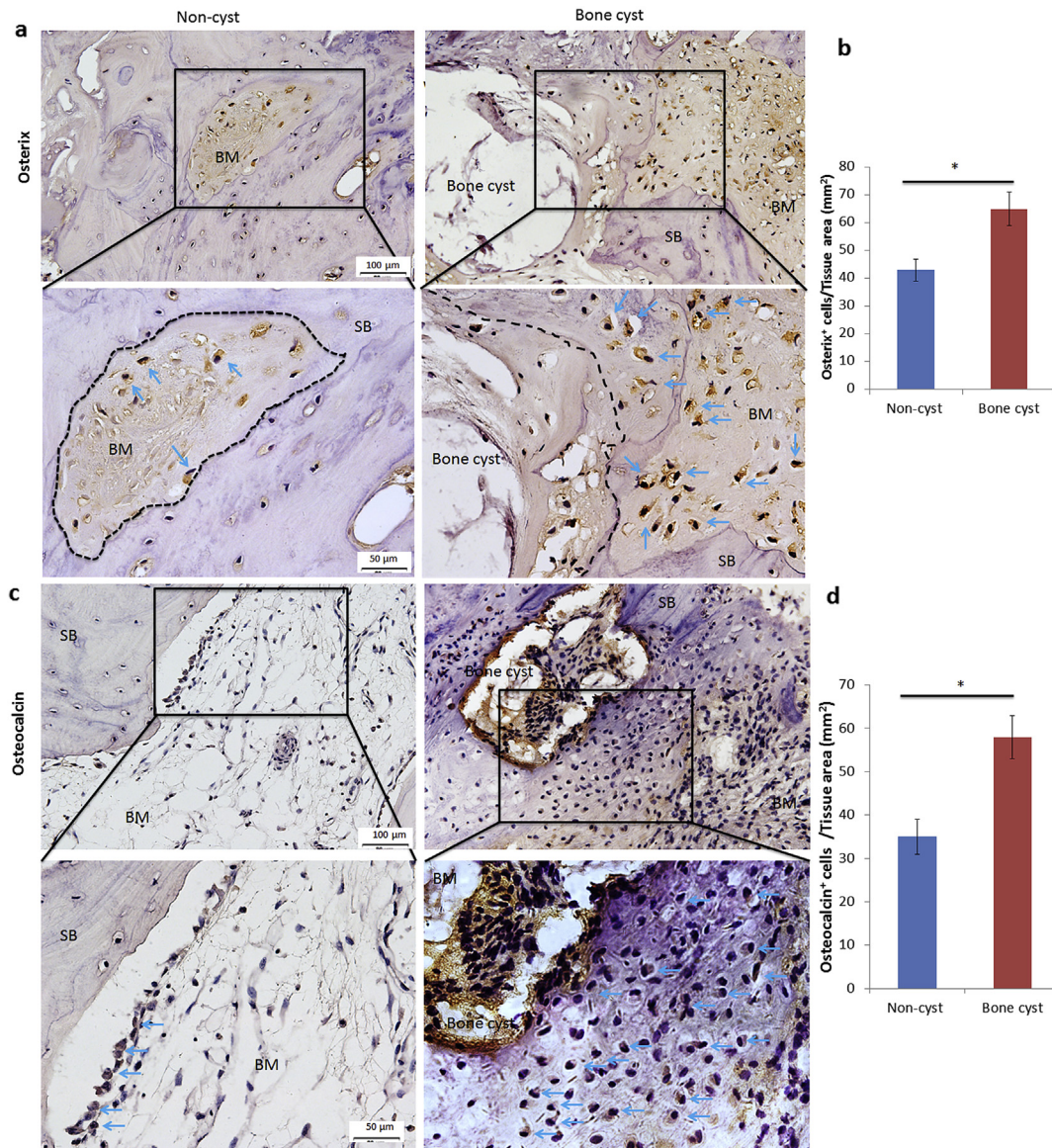


**Fig. 6. Activity of Osterix<sup>+</sup> osteoprogenitors and Osteocalcin<sup>+</sup> osteoblasts in subchondral bone without or with bone cysts.** (a) Compared with the non-cyst group, more Osterix<sup>+</sup> osteoprogenitors (arrows) were observed in the bone cyst group, and they tended to be located in the bone marrow adjacent to the bone cyst. Note the presence of a large bone cyst. (b) Quantitative analysis showed a significantly higher number of Osterix<sup>+</sup> osteoprogenitors in the bone cyst group, indicating higher level of osteogenesis compared with the non-cyst group. (c) Compared with the non-cyst group, more Osteocalcin<sup>+</sup> osteoblasts (arrows) were noted in the bone cyst group. The Osteocalcin<sup>+</sup> osteoblasts tended to be located adjacent to the bone cyst. (d) Quantitative analysis showed significantly higher number of Osteocalcin<sup>+</sup> osteoblasts in the bone cyst group, indicating a higher level of bone formation. \* =  $P < 0.05$ .

The 3-D micro-CT and histology analyses were consistent with each other and illustrated that the wall of the SBCs is sclerotic, with increased bone volume and Tb.N (Supplementary Fig. 2). The positive relationships of these values with SBC volume suggest increased bone formation (Table 1). The finding of lower SMI indicates that trabeculae around the SBCs were more plate-like compared with the non-cyst groups. This finding is consistent with previous human studies<sup>32,33</sup>. Plate-like trabeculae reflect higher mechanical strength and stiffness than rod-like trabeculae<sup>33,34</sup>. Therefore, our results suggest that trabeculae surrounding SBCs may have increased stiffness. No significant differences were found in BMD, DA, or Conn.D between the two groups. However, this may be mainly due to the large variability within the specimens in bone cyst group.

No significant differences in bone structure were found between the matched and peri-cyst subregions, suggesting that bone

structure changes are localized to the areas immediately adjacent to SBCs. There were significant differences in BMD between the cyst and peri-cyst subregions, indicating that subchondral bone surrounding SBCs is not only sclerotic but contains less mineral, and is in accordance with results from a previous study of hip OA<sup>25</sup>. The reduced BMD of subchondral bone surrounding SBCs may thus also have mechanical consequences. The determination of mechanical properties will be required in future studies.

Safranin O and Fast Green staining showed proteoglycan-containing fibrocartilaginous tissue at the edge of SBCs and in cyst cavities. Fibrocartilaginous tissue is heterotopic in some of the end-staged OA subchondral bone<sup>35</sup>. It is considered to carry out tissue regeneration by synthesizing collagen Type I but not collagen Type II which is typical for healthy cartilage<sup>35</sup>. Further immunohistochemical staining of SOX9—a biomarker for the chondrogenic phase during endochondral bone formation, which has been



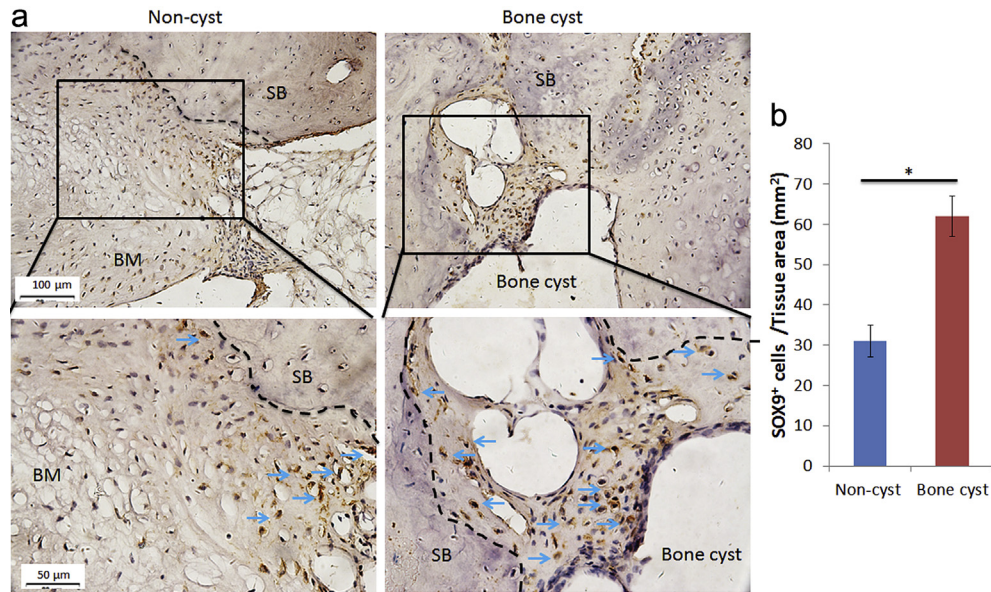


**Fig. 7. Immunohistochemical staining of SOX9 in subchondral bone without or with bone cysts.** (a) Compared with the non-cyst group, more cells with positive staining of SOX9—a biomarker of chondrogenic phase of endochondral bone formation—were defined in bone cyst group (blue arrows). The SOX9<sup>+</sup> cells were mainly located at the wall of bone cyst. (b) Quantitative analysis showed a significantly higher number of SOX9<sup>+</sup> cells in the bone cyst group, indicating elevated endochondral bone formation than the non-cyst group. \* =  $P < 0.05$ .

detected during fracture healing<sup>36</sup> and heterotopic ossification<sup>30</sup>—revealed that SOX9<sup>+</sup> cells aggregate around the cyst wall (Fig. 7). Consistently, higher numbers of Osteocalcin<sup>+</sup> osteoblasts were detected surrounding the bone cyst wall compared with the non-cyst group. The above findings suggest that endochondral bone formation occurred at the cyst wall, which indicates abnormal subchondral bone remodeling.

On the other hand, immunohistochemical analysis showed elevated activity of Osterix<sup>+</sup> osteoprogenitors surrounding SBCs (Fig. 6), suggesting increased osteogenic differentiation of bone marrow mesenchymal bone marrow stem cells (MSCs). Clusters of Osterix<sup>+</sup> osteoprogenitors in subchondral bone marrow, and consequent increased bone formation, has been characterized in knee OA pathogenesis in our previous studies<sup>3,4</sup>. Therefore, our finding suggests that increased osteogenic differentiation of MSCs partly contributes to the increased bone turnover surrounding SBCs.

There are several limitations of this study. First, this is a cross-sectional study. Thus, we were not able to monitor subchondral bone turnover and cartilage damage during cyst development longitudinally. Second, the patients recruited in this study had moderate-to-severe knee OA. Therefore, the results could not represent the conditions in earlier stages of human OA. Third, in the present study, the bone and cartilage samples were extracted from the center of the load-bearing area of the tibial plateau. However, SBCs and the corresponding bone turnover and cartilage degradation in other regions of the tibial plateau may differ. Fourth, reports from arthroplasty registries showed that gender distribution of knee OA patients varies among different countries<sup>37</sup>. In a South Korea study, female patients comprised as high as 88.1–88.9% of the total sample of knee OA patients<sup>38</sup>. Similarly, in the authors' hospital, it has been reported that the female patients comprised 79.2–85.5% of the total sample of knee OA patients<sup>39</sup>. In the current study, 88.7% of the patients were female. Thus, the gender of patients was skewed toward females, and males were underrepresented. In addition, this skewed gender distribution, together with other characteristics, limits the interpretation of the results to certain cohorts of patients, such as Asians vs other ethnic groups.

Last but not least, only SBCs with diameters greater than 1 mm were included in this study, because it is difficult to precisely differentiate between very small SBCs and bone marrow space using micro-CT<sup>25,26</sup>. Thus, this study may underestimate the effects of SBCs, and lead to the relatively weak relationships ( $r^2 < 0.30$ ) between SBC volume and parameters of subchondral bone and cartilage damage.

Taken together, we found that SBC regions in human OA knees are foci of increased bone remodeling and altered structure, and are spatially associated with articular cartilage degradation. These results imply the biomechanical link between SBC formation and cartilage damage. Our further analyses provide a “bone remodeling” model for SBC formation: due to mechanical stimulus<sup>40</sup> or/and biochemical micro-environment changes<sup>1,2</sup>, the remodeling of subchondral bone is activated. Necrotic bone fragments are phagocytosed by osteoclasts, creating the cyst cavity. Meanwhile, bone formation is enhanced by endochondral bone formation as well as increased activity of osteoprogenitors and osteoblasts, resulting in a sclerotic cyst wall. This model favors the “bony contusion theory”<sup>16,17</sup>. Thus, our findings prompt the need for a longitudinal study to confirm the “bone remodeling” model for SBC formation and its causal relationship with articular cartilage degeneration.

#### Author contributions

All authors were involved in drafting the article for important intellectual content, and all authors approved the final version to be published.

*Study conception and design:* YC, FL, HP, XC, XEG, WWL.

*Acquisition of data:* YC (Clinical, micro-CT and histology data), TW (Micro-CT data), MG and WZ (histology data).

*Analysis and interpretation of data:* YC, TW, FL, HP, XC, XEG, WWL.

#### Conflict of interests

The authors declare that they have no competing interests.

## Acknowledgments

The work was supported by Ng Chun-Man Foundation, National Natural Science Foundation of China (NSFC 81270967# and 81300719#), Shenzhen Peacock Project (No. 110811003586331) and the Research Grant Council of Hong Kong (HKU715213).

## Supplementary data

Supplementary data related to this article can be found at <http://dx.doi.org/10.1016/j.joca.2015.07.012>.

## References

- Loeser RF, Goldring SR, Scanzello CR, Goldring MB. Osteoarthritis: a disease of the joint as an organ. *Arthritis Rheum* 2012;64:1697–707.
- Lories RJ, Luyten FP. The bone-cartilage unit in osteoarthritis. *Nat Rev Rheumatol* 2011;7:43–9.
- Zhen G, Wen C, Jia X, Li Y, Crane JL, Mears SC, et al. Inhibition of TGF-beta signaling in mesenchymal stem cells of subchondral bone attenuates osteoarthritis. *Nat Med* 2013;19:704–12.
- Wang T, Wen CY, Yan CH, Lu WW, Chiu KY. Spatial and temporal changes of subchondral bone proceed to microscopic articular cartilage degeneration in guinea pigs with spontaneous osteoarthritis. *Osteoarthritis Cartilage* 2013;21:574–81.
- Burr DB, Gallant MA. Bone remodelling in osteoarthritis. *Nat Rev Rheumatol* 2012;8:665–73.
- Radin EL, Rose RM. Role of subchondral bone in the initiation and progression of cartilage damage. *Clin Orthop Relat Res* 1986;34–40.
- Plewes LW. Osteo-arthritis of the hip. *Br J Surg* 1940;27:682–95.
- Forestier J, Robert P. X-Ray diagnosis in chronic arthritis: (section of radiology). *Proc R Soc Med* 1940;33:707–24.
- Crema MD, Roemer FW, Marra MD, Guermazi A. MR imaging of intra- and periarticular soft tissues and subchondral bone in knee osteoarthritis. *Radiol Clin North Am* 2009;47:687–701.
- Crema MD, Roemer FW, Zhu Y, Marra MD, Niu J, Zhang Y, et al. Subchondral cystlike lesions develop longitudinally in areas of bone marrow edema-like lesions in patients with or at risk for knee osteoarthritis: detection with MR imaging—the MOST study. *Radiology* 2010;256:855–62.
- Raynauld JP, Martel-Pelletier J, Berthiaume MJ, Abram F, Choquette D, Haraoui B, et al. Correlation between bone lesion changes and cartilage volume loss in patients with osteoarthritis of the knee as assessed by quantitative magnetic resonance imaging over a 24-month period. *Ann Rheum Dis* 2008;67:683–8.
- Kornaat PR, Bloem JL, Ceulemans RY, Riyazi N, Rosendaal FR, Nelissen RG, et al. Osteoarthritis of the knee: association between clinical features and MR imaging findings. *Radiology* 2006;239:811–7.
- Kumar D, Wyatt CR, Lee S, Nardo L, Link TM, Majumdar S, et al. Association of cartilage defects, and other MRI findings with pain and function in individuals with mild-moderate radiographic hip osteoarthritis and controls. *Osteoarthritis Cartilage* 2013;21:1685–92.
- Tanamas SK, Wluka AE, Pelletier JP, Martel-Pelletier J, Abram F, Wang Y, et al. The association between subchondral bone cysts and tibial cartilage volume and risk of joint replacement in people with knee osteoarthritis: a longitudinal study. *Arthritis Res Ther* 2010;12:R58.
- Landells JW. The bone cysts of osteoarthritis. *J Bone Joint Surg Br* 1953;35-B:643–9.
- Ondrouch AS. Cyst formation in osteoarthritis. *J Bone Joint Surg Br* 1963;45:755–60.
- Rhaney K, Lamb DW. The cysts of osteoarthritis of the hip; a radiological and pathological study. *J Bone Joint Surg Br* 1955;37-b:663–75.
- Pouders C, De Maeseneer M, Van Roy P, Gielen J, Goossens A, Shahabpour M. Prevalence and MRI-anatomic correlation of bone cysts in osteoarthritic knees. *AJR Am J Roentgenol* 2008;190:17–21.
- McErlain DD, Ulici V, Darling M, Gati JS, Pitelka V, Beier F, et al. An *in vivo* investigation of the initiation and progression of subchondral cysts in a rodent model of secondary osteoarthritis. *Arthritis Res Ther* 2012;14:R26.
- Altman R, Asch E, Bloch D, Bole G, Borenstein D, Brandt K, et al. Development of criteria for the classification and reporting of osteoarthritis. Classification of osteoarthritis of the knee. Diagnostic and Therapeutic Criteria Committee of the American Rheumatism Association. *Arthritis Rheum* 1986;29:1039–49.
- Kellgren JH, Lawrence JS. Radiological assessment of osteoarthrosis. *Ann Rheum Dis* 1957;16:494–502.
- Gossec L, Jordan JM, Mazuca SA, Lam MA, Suarez-Almazor ME, Renner JB, et al. Comparative evaluation of three semi-quantitative radiographic grading techniques for knee osteoarthritis in terms of validity and reproducibility in 1759 X-rays: report of the OARSI-OMERACT task force. *Osteoarthritis Cartilage* 2008;16:742–8.
- Sharma L, Chmiel JS, Almagor O, Felson D, Guermazi A, Roemer F, et al. The role of varus and valgus alignment in the initial development of knee cartilage damage by MRI: the MOST study. *Ann Rheum Dis* 2013;72:235–40.
- Wen CY, Chen Y, Tang HL, Yan CH, Lu WW, Chiu KY. Bone loss at subchondral plate in knee osteoarthritis patients with hypertension and type 2 diabetes mellitus. *Osteoarthritis Cartilage* 2013;21:1716–23.
- Chiba K, Nango N, Kubota S, Okazaki N, Taguchi K, Osaki M, et al. Relationship between microstructure and degree of mineralization in subchondral bone of osteoarthritis: a synchrotron radiation microCT study. *J Bone Miner Res* 2012;27:1511–7.
- Chiba K, Burghardt AJ, Osaki M, Majumdar S. Three-dimensional analysis of subchondral cysts in hip osteoarthritis: an *ex vivo* HR-pQCT study. *Bone* 2014;66:140–5.
- Hahn M, Vogel M, Pompesius-Kempa M, Delling G. Trabecular bone pattern factor—a new parameter for simple quantification of bone microarchitecture. *Bone* 1992;13:327–30.
- Hildebrand T, Rueggsegger P. Quantification of bone microarchitecture with the structure model index. *Comput Methods Biomech Biomed Engin* 1997;1:15–23.
- Pritzker KP, Gay S, Jimenez SA, Ostergaard K, Pelletier JP, Revell PA, et al. Osteoarthritis cartilage histopathology: grading and staging. *Osteoarthritis Cartilage* 2006;14:13–29.
- Lin L, Shen Q, Xue T, Yu C. Heterotopic ossification induced by Achilles tenotomy via endochondral bone formation: expression of bone and cartilage related genes. *Bone* 2010;46:425–31.
- Tang Y, Wu X, Lei W, Pang L, Wan C, Shi Z, et al. TGF-beta1-induced migration of bone mesenchymal stem cells couples bone resorption with formation. *Nat Med* 2009;15:757–65.
- Ding M, Odgaard A, Danielsen CC, Hvid I. Mutual associations among microstructural, physical and mechanical properties of human cancellous bone. *J Bone Joint Surg Br* 2002;84:900–7.
- Ding M, Odgaard A, Hvid I. Changes in the three-dimensional microstructure of human tibial cancellous bone in early osteoarthritis. *J Bone Joint Surg Br* 2003;85:906–12.

34. Wang J, Zhou B, Liu XS, Fields AJ, Sanyal A, Shi X, *et al.* Trabecular plates and rods determine elastic modulus and yield strength of human trabecular bone. *Bone* 2014;72c:71–80.
35. Tesche F, Miosge N. New aspects of the pathogenesis of osteoarthritis: the role of fibroblast-like chondrocytes in late stages of the disease. *Histol Histopathol* 2005;20:329–37.
36. Soung do Y, Talebian L, Matheny CJ, Guzzo R, Speck ME, Lieberman JR, *et al.* Runx1 dose-dependently regulates endochondral ossification during skeletal development and fracture healing. *J Bone Miner Res* 2012;27:1585–97.
37. Robertsson O, Bizjajeva S, Fenstad AM, Furnes O, Lidgren L, Mehnert F, *et al.* Knee arthroplasty in Denmark, Norway and Sweden: a pilot study from the Nordic Arthroplasty Register Association. *Acta Orthop* 2010;81:82–9.
38. Kim HA, Kim S, Seo YI, Choi HJ, Seong SC, Song YW, *et al.* The epidemiology of total knee replacement in South Korea: national registry data. *Rheumatology (Oxford)* 2008;47:88–91.
39. Yan CH, Chiu KY, Ng FY. Total knee arthroplasty for primary knee osteoarthritis: changing pattern over the past 10 years. *Hong Kong Med J* 2011;17:20–5.
40. Cox LG, van Donkelaar CC, van Rietbergen B, Emans PJ, Ito K. Alterations to the subchondral bone architecture during osteoarthritis: bone adaptation vs endochondral bone formation. *Osteoarthritis Cartilage* 2013;21:331–8.